

Molecular Dynamics Studies of Dog Prion Protein Wild-type and Its D159N Mutant

Jiapu Zhang^{ab*}

^a*Molecular Model Discovery Laboratory, Department of Chemistry & Biotechnology, Faculty of Science, Engineering & Technology, Swinburne University of Technology, Hawthorn Campus, Hawthorn, Victoria 3122, Australia;*

^b*Graduate School of Sciences, Information Technology and Engineering & Centre of Informatics and Applied Optimisation, Faculty of Science, The Federation University Australia, Mount Helen Campus, Mount Helen, Ballarat, Victoria 3353, Australia;*

^{*}*Tel: +61-3-9214 5596, +61-3-5327 6335; jiapuzhang@swin.edu.au, j.zhang@federation.edu.au*

Abstract: *Prion diseases (e.g. ‘mad cow’ disease in cattle, chronic wasting disease in deer and elk, Creutzfeldt-Jakob disease in humans) have been a major public health concern affecting humans and almost all animals. However, dogs are strongly resistant to prion diseases. Recently, through transgenic techniques, it was reported that the single (surface) residue D159 is sufficient to confer protection against protein conformational change and pathogenesis, thus provides conformational stability for dog prion protein (Neurobiology of Disease 95 (November 2016) 204-209). This paper studies dog prion protein wild-type and D159N mutant through molecular dynamics (MD) techniques. Our MD results reveal sufficient structural informatics on the residue at position 159 to understand the mechanism underlying the resistance to prion diseases of dogs.*

Key words: *prion diseases; immunity of dogs; key residue D159; wild-type and mutant; molecular dynamics.*

1 Introduction

Unlike bacteria and viruses, which are based on DNA and RNA, prions are unique as disease-causing agents since they are misfolded proteins. Prions propagate by deforming harmless, correctly folded proteins into copies of themselves. The misfolding is irreversible. Prions attack the nervous system of the organism, causing an incurable, fatal deterioration of the brain and nervous system until death occurs. Some examples of these diseases are ‘mad cow’ disease (BSE) in cattle, chronic wasting disease (CWD) in deer and elk, and Creutzfeldt-Jakob disease (CJD) in humans.

Not every species is affected by prion disease. Rabbits, water buffalo, horses, and dogs are resistant to prion diseases [22]. The research question arises: What are reasons allowing the protein of a resistant species to retain its folding? For rabbit normal cellular prion protein (PrP^C, where the structural region of a PrP^C consists of β -strand 1 (β 1), α -helix 1 (α 1 or H1), β -strand 2 (β 2), α -helix 2 (α 2 or H2), α -helix 3 (α 3 or H3), and the loops linking them each other), multiple amino acid residues G99, M108, S173, I214, together inhibit formation of its abnormal isoform [17]. For dog PrP, D159 is the key protective residue that provides conformational stability and confers protection against prions, suggesting that a single amino acid D159 is sufficient to prevent

PrP conformational change and pathogenesis [15]. This paper will specially study the residue D159 of dog PrP from the protein structural dynamics point of view.

First, let us review some known literatures on dog PrP (and we particularly focus on its structural bioinformatics). There are a lot of literatures reporting dogs (and other canines) are rare animals being resistant to prion diseases, for examples [2, 3, 5, 6, 11, 13, 14, 16, 19, 24].

- Early in 1994, it was found that not a single case of prion disease has been described among dogs through the exposure of dogs to prions (being fed prion-infected pet food) [6].
- In 1999, it was reported that two differences between feline and canine PrP sequences, at codons 187 and 229, both involve substitutions to Arg residues which, together with the His-Arg substitution at codon 177 common to cat and dog, would increase the total positive surface charge on the molecule - this might in turn affect the potential intermolecular interactions critical for cross-species transmission of prion disease [19].
- In 2004, it was reported that the three substitutions in positions 108, 164, and 182 are unique to the canine species and are thus candidates for causing a substantial species barrier, and dogs are among the few mammals that neither contain Asn at position 164 (or 159) nor His at position 182 (or 177) [8, 9].
- In 2005, the NMR structure of dog PrP was released (PDB entry 1XYK) and it was reported that the residues at positions 159 and 177 have unique charge distribution patterns on the front as well as the back side of dog PrP^C [10]. The residue D159 (less defined by NMR) is proposed to change the surface charge [10] due to its sticking out acidic side chain.
- In 2006, the open reading frame of the prion protein (Prnp) gene from 16 Pekingese dogs was cloned and screened for polymorphisms [20]. One nucleotide polymorphism (G489C) was found; the G to C nucleotide substitution results in a glutamic to aspartic acid change at codon 163; E/D163 and asparagine 107 in canine prion protein genes were replaced by asparagine and serine, respectively, in all the prion protein genes examined [20].
- In 2008, transmission experiments in Madin Darby canine kidney (MDCK) cells showed they do not replicate human CJD prions and mouse (infected with scrapie) prions [13], supporting the resistance of dogs to prions. Human PrP^C is selectively targeted to the apical side of the MDCK [1].
- In 2009, Onizuka (2009) reported the substitutions N104G and S107N have the biggest impact to the conformational transition and stability of dog PrP [12]. In 2009, it was reported in [18] that the three substitutions in positions 107, 163, and 181 are unique to the Arctic fox and dog, and these substitutes might be associated with susceptibility and species barriers in prion diseases.

- In 2010, Khan et al. (2010) found that at pH 4.0 dogs have the lowest concentration of β intermediate state compared with hamsters, mice, rabbits and horses [5, 14] - this can be adopted in evaluating the prion disease susceptibility of each species (hamster>mouse>rabbit>horse>dog) [2, 5, 14].
- In 2013, Hasegawa et al. (2013) reported that there are large differences in local structural stabilities between canine and bovine PrP, and this appearance might link diversity in susceptibility to BSE prion infection [3].
- In 2015, a survey of prnp genes implied that the prion disease resistant canines harbor amino acids DRK in positions 159, 177, and 185 [11]. Arg177 in H2 of dog PrP also causes unique charge distribution patterns on the front and the back side of dog PrP^C [10], but Arg177 are positively charged residue that should have minor effects on PrP structure and surface charge [15], because the sequence of the rigid $\beta 2$ - $\alpha 2$ loop in the dog is identical to mouse PrP, indicating that this region does not contribute to the conformational stability of dog PrP [2].

In 2016, Sanchez-Garcia et al. (2016) reported that a single amino acid (D159) from the dog PrP suppresses the toxicity of the mouse PrP in *Drosophila* [15] and their laboratory experience suggested that a single D159 substitution is sufficient to prevent PrP conformational change and pathogenesis [15]. D159 is a unique amino acid found in PrP from dogs and other canines that was shown to alter surface charge. The acidic amino acid D159 is on the $\alpha 1$ - $\beta 2$ loop and exposed on the surface of dog PrP, resulting in increased negative charge [15]. The $\beta 1$ - $\alpha 1$ and $\alpha 1$ - $\beta 2$ loops interact more closely in dog PrP than in susceptible animals thus the subtle changes in the orientation of the side chains and the closer loops may affecting the stability of the β -sheet [3, 10] - this might explain the poor NMR resolution of residue D159. The mutation N159 will create a neutral surface that extends over the surface of the two loops (i.e. the $\beta 1$ - $\alpha 1$ loop and the $\alpha 1$ - $\beta 2$ loop) and H2 [15]. In the D159 region there only harbors one non-sense pathogenic mutation Q160X, however, this critical domain should be investigated in more details, because the identification of $\alpha 1$ - $\beta 2$ loop-binding proteins are expected to reveal clues about the molecular mechanisms and the extrinsic factors mediating PrP conversion from soluble normal prion protein PrP^C (predominant in α -helices) to insoluble diseased infectious prions PrP^{Sc} (rich in β -sheets) [15]. It has been proposed that this change in surface charge will result in altered interactions with other proteins, possibly proteins that contribute to PrP conversion [15]. The $\alpha 1$ - $\beta 2$ loop is highly conserved among mammals but only dog PrP possesses the unique acidic residue D159 suggesting that D159 plays a role in providing *global* stability to dog PrP [2]. We also once reported that the residue at position 159 is unique in dog PrP^C [21, 22, 23]. This paper will continue our research on the molecular dynamics (MD) studies of dog PrP, especially on the MD studies of its D159N mutant and their comparisons.

The rest of this paper is organized as follows. In Section 2 we will give the MD simulation materials and methods. Section 3 will presents the MD results and their analyses (where surface charge distributions are specially focused to analyze the MD trajectories). After the Results and Discussions section, some Concluding Remarks (revealed from the MD to understand the mechanism underlying the resistance to prion

diseases of dogs) will be given in the last section of this paper.

2 Materials and Methods

The MD simulation materials and methods are completely as the ones of [21, 22, 23]. The D159N mutant model used in this study was constructed by one mutation D159N at position 159 using the NMR structure 1XYK.pdb of dog PrP (121–231), where the NMR experimental temperature is 293 K (i.e. the room temperature), pH value is 4.5, and pressure is AMBIENT. To neutralize the MD systems by sodium ions, 2 Na⁺ ions were added to the wild-type, and 1 Na⁺ ion was added to the D159N mutant (because the residue Asn is without charge). 1XYK.pdb has 8 Arg⁺ residues and 4 Lys⁺ residues (and 2 His⁺ residues), 6 Asp⁻ residues and 8 Glu⁻ residues, two salt bridges D144.OD1–R+148.NH1/2, D178.OD2–R+164.NE/NH2 and one cation- π interaction R164.CD–Y128 detected by FirstGlance in Jmol (bioinformatics.org/firstglance/fgij/). This paper uses Maestro 9.7 2014-1 (Academic use only) free package to draw the Poisson-Boltzmann electrostatic potential surface charges of the external polarization: we choose $\epsilon_{\text{di}} = 1.0$ as the solute dielectric constant, $\epsilon_{\text{di}} = 80.0$ as the solvent dielectric constant, 12 Å as the solvent radius, and 300 K as the Temperature: EPS mapped on molecular surface is chosen.

Electrostatic potential surfaces are valuable in structure-based/computer-aided drug design because they help in optimization of electrostatic interactions between the protein and the ligand. These surfaces can be used to compare different inhibitors with substrates or transition states of the reaction. To study the surface charge of a residue and its local and global impacts should firstly consider the salt bridges (SBs) it linked with [25]. SBs are calculated by oppositely charged atoms that are within 6.5 Å and are not directly hydrogen-bonded. It should be the average charge calculated per residue or the specific atom charge of the residue. The donor residues involved are Asp⁻, Glu⁻, and the acceptor residues involved are Lys⁺, Arg⁺, His⁺, and the real computed distance is within 6.5 Å in Amber package.

3 Results and Discussions

Firstly, we see the secondary structure changes of the D159N mutant and of the wild-type during the whole 30 ns’ molecular movement. By Fig. 1, we may see what we want: for $\beta 1$ and $\beta 2$, the wild-type has the clear extended β -strand (participates in β -ladder) structure (with the occupied rate 3.66% during the whole 30 ns), but the D159N mutant has changed into β -bridge structures (occupied rate 0.34% during 30 ns). This performance implied to us the mutation D159N has clearly changed the PrP structure in domains of $\beta 1$, the $\beta 1$ - $\alpha 1$ loop, H1, the $\alpha 1$ - $\beta 2$ loop, $\beta 2$, and the $\beta 2$ - $\alpha 2$ loop. The mutation made the stable wild-type structure (before H2) become unstable.

Secondly, we see the SBs of the D159N mutant and of the wild-type during the 30 ns’ MD simulations. As we previously reported [21, 22, 23] the SB D178–R164 like a taut bow string of the $\beta 2$ - $\alpha 2$ loop was broken by the D159N mutation (Fig. 2). This implies to us that residue R164 spans only 4 residues from residue D159, and residue

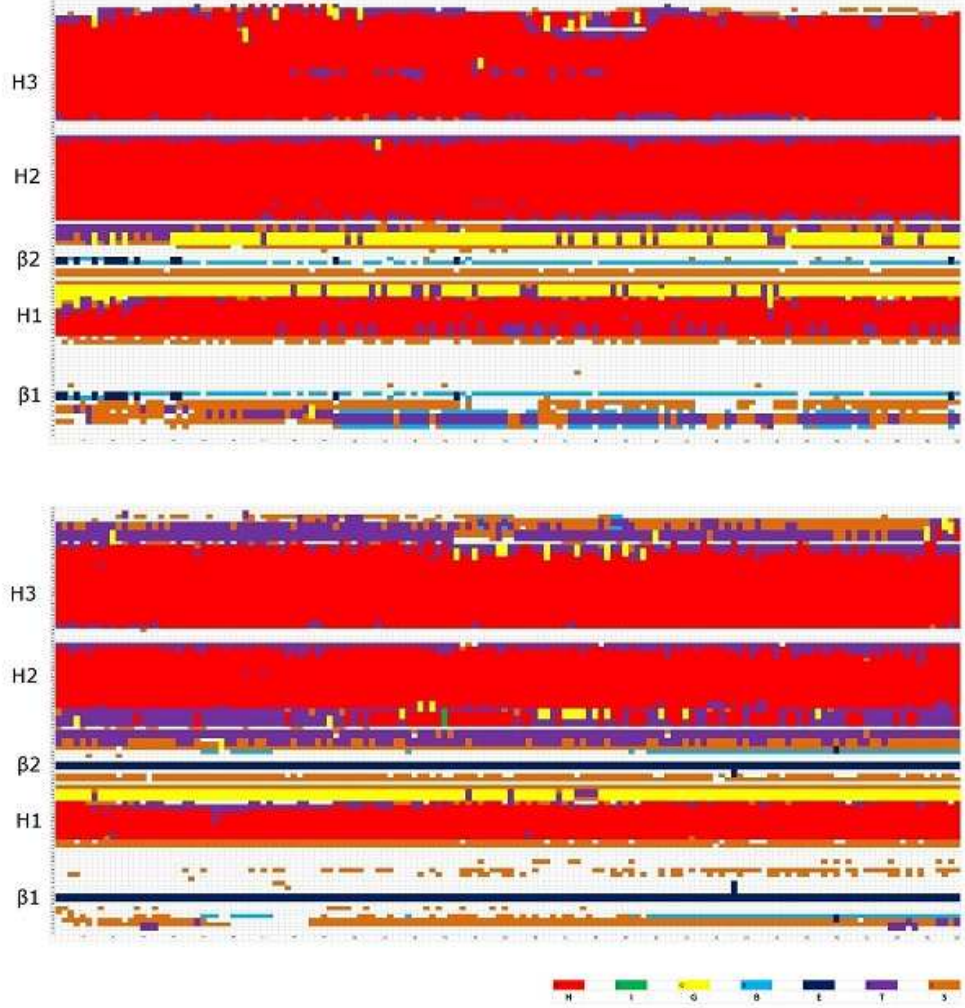


Figure 1: Secondary Structure graph for dog PrP D159N mutant and dog PrP wild-type (from up to down) at 300 K under neutral pH environment (x-axis: time (0-30 ns), y-axis: residue number; red: α -helix (H), blue: β -sheet (E), where H = α -helix, B = residue in isolated β -bridge, E = extended strand, participates in β -ladder, G = 3-helix (3_{10} helix), I = 5 helix (π -helix), T = hydrogen bonded turn, and S = bend).

D159 has a rather impact on the local structure. The SB D159–R136 at residue D159, with occupied rate 92.48% during 30 ns, was broken in the D159N mutant; this SB keeps the β 1- α 1 loop apart from the α 1- β 2 loop. This shows the stabilizing effect of D159 in dog PrP to affect the both locally and globally unusual charge distribution of NMR structure of dog PrP. Furthermore, we want to see and analyze all the SBs during the whole 30 ns (Tab. 1). Seeing Table 1, we may know that “<” shows the local impact of the D159N mutation which made the weaker of the wild-type’s SBs such as D159–R+136, E211–R+177, D147–R+151, D178–R+164, E146–K+204, E196–R+156, D202–R+156, H+187–R+156, E152–R+148, and “*” implies the global impact of the D159N mutation which made weaker of the wild-type’s SBs. To understand better the

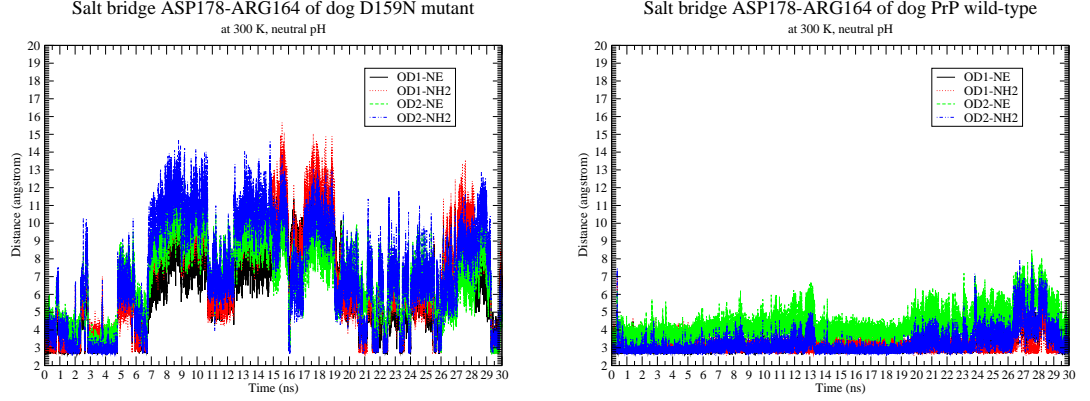


Figure 2: The SB D178–R164 of the D159N mutant (with occupied rate 9.25% during the whole 30 ns of MD) and of the wild-type (with occupied rate 49.43% during the whole 30 ns of MD) at 300 K under neutral pH condition..

Table 1: All SBs of the D159N mutant and of the wild-type at 300 K, neutral pH value during the whole 30 ns’ MD simulations:

Salt Bridges (SBs)	D159N mutant (% occupied rate)		Wild-type (% occupied rate)	In PrP, where?
D147–R+148	100.00		100.00	in H1
D178–R+177	99.82		99.57	in H2
E223–K+220	98.56		41.85	in H3
E207–K+204	98.43		96.13	in H3
E211–R+208	97.71	*	99.13	in H3
D144–R+148	93.72		53.47	in H1
D147–H+140	82.21		72.37	H1 – β 1- α 1-loop
E207–R+208	76.43		44.87	in H3
E196–K+194	75.98		59.57	in α 2- α 3-loop
E152–R+148	53.16	<	53.52	in H1
E152–R+151	51.11		43.63	in H1
H187–R+156	42.75	<	44.74	H2 – α 1- β 2-loop
E211–R+177	30.02	<	45.91	H3 – H2
E221–K+220	14.07	*	53.71	in H3
D147–R+151	11.41	<	25.68	in H1
D202–H+187	9.25		1.19	H3 – H2
D178–R+164	7.82	<	49.43	H2 – β 2- α 2-loop
D167–R+228	4.22			β 2- α 2-loop – H3
E146–K+204	2.96	<	24.73	H1 – H3
H187–K+185	2.31		0.46	in H2
E196–R+156	0.43	<	16.20	α 2- α 3-loop – α 1- β 2-loop
H140–R+151	0.20	*	0.29	β 1- α 1-loop – H1
E200–K+204	0.03	*	0.21	in H3
E196–H+187	0.03	*	0.09	α 2- α 3-loop – H2
E221–R+228	0.02			in H3
D159–R+136		<	92.48	α 1- β 2-loop – β 1- α 1-loop
D202–R+156		<	8.20	H3 – α 1- β 2-loop
E223–R+228		*	0.15	in H3
D144–H+140		*	0.05	in β 1- α 1-loop
H140–R+228		*	0.01	β 1- α 1-loop – H3

above SBs, we illuminate the surface charge distributions of the 30 ns’ average structure of the D159N mutant and the wild-type respectively (Fig. 3). From Fig. 3, we see that the D159N mutation made the negative charges and the positive charges redistributed

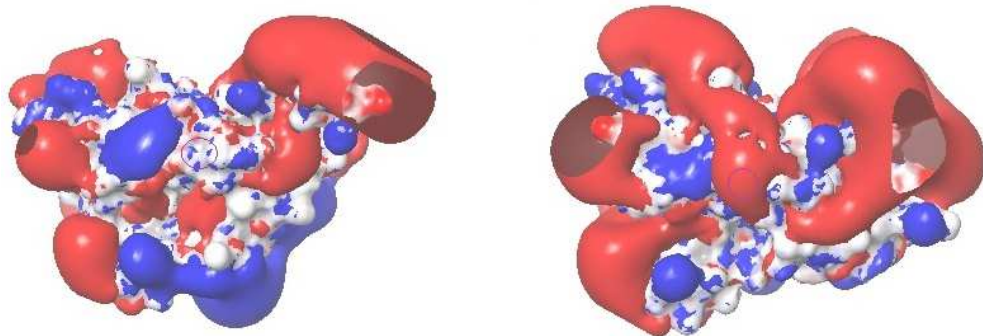


Figure 3: *Surface charge distributions of the 30 ns' average structure. Left: The N159 mutant of dog PrP; right: The wild-type of dog PrP. The circles indicate charge differences originating at position 159. Red, blue, and white indicate the negative, positive charges and uncharged respectively.*

around the residue at position 159; however, the negative charges covering H1 and the tail of H3 are not changed very much - this implies to us we had better not seek drug target(s) from H1 or the tail of H3.

Thirdly, we will give a brief overview of the changes of some hydrogen bonds (HBs) and hydrophobic interactions (HYDs) made by the D159N mutation. In view of the number of HBs, we cannot say differences between the D159N mutant and the wild-type; however, the HBs listed in Tab. 2 contribute to the structural stability of wild-type dog PrP more than of the D159N mutant. We may see from Tabs. 1~2 that (i) D202-R+156 and E223-R+228 are two polar contacts for the wild-type, but the D159N mutant is without these polar contacts; (ii) D147-H+140, E211-R+177, D147-R+151, D178-R+164 are four strong polar contacts for the wild-type but weaker for the D159N mutant. Regarding hydrophobic interactions (HYDs), throughout the whole 30 ns' MD simulations, the D159N mutation has a local impact - it made HYD M213-V161 become weaker than in the wild-type, and has global impacts - it made V215-M213 and V209-I205 become weaker than in the wild-type. Around the residue at position 159, we find there are one π - π stacking F141-Y150 and one π -cation Y164-R164 in the D159N mutant and the π - π stacking F141-Y150 in the wild-type PrP through the whole 30 ns' protein movement. We also noticed that GN8 [7, 4], an antiprion drug fixing the distance between N159 and E196 being 1.54 Å, was designed at the position 159 - this might show the importance of the PrP residue at position 159.

4 Concluding Remarks

The mutation D159N of dog PrP had profound effects on protein structure of dog PrP: (1) it altered the surface charge distribution, both locally and globally, (2) it reduced the stability of the tertiary structure of dog PrP, and (3) it increased the mobility of dog PrP structure before H2. The MD studies of this paper confirmed these three findings and emphasized the contribution of the single residue D159 in dictating the global (and

local) charge distribution and structural stability of dog PrP. This paper presented detailed sufficient structural informatics on the residue at position 159 to understand the mechanism underlying the resistance to prion diseases of dogs; this may be useful for the medicinal treatment of prion diseases.

Acknowledgments

This research was supported by a Victorian Life Sciences Computation Initiative (VLSCI) grant numbered FED0001 on its Peak Computing Facility at the University of Melbourne, an initiative of the Victorian Government (Australia).

References

- [1] De Keukeleire B, Donadio S, Micoud J, Lechardeur D, Benharouga M (2007) Human cellular prion protein hPrP^C is sorted to the apical membrane of epithelial cells. *Biochem Biophys Res Commun* 354(4):949–54.
- [2] Fernandez-Funez P, Zhang Y, Sanchez-Garcia J, Jensen K, Zou WQ, Rincon-Limas DE (2011) Pulling rabbits to reveal the secrets of the prion protein. *Commun Integr Biol* 4(3):262–6.
- [3] Hasegawa K, Mohri S, Yokoyama T (2013) Comparison of the local structural stabilities of mammalian prion protein (PrP) by fragment molecular orbital calculations *Prion* 7(2):185–91.
- [4] Hosokawa-Muto J, Kimura T, Kuwata K (2012) Respiratory and cardiovascular toxicity studies of a novel antiprion compound, GN8, in rats and dogs. *Drug Chem Toxicol* 35(3):264–71.
- [5] Khan MQ, Sweeting B, Mulligan VK, Arslan PE, Cashman NR, Pai EF, Chakrabartty A (2010) Prion disease susceptibility is affected by beta-structure folding propensity and local side-chain interactions in PrP. *Proc Natl Acad Sci USA* 107(46):19808–13.
- [6] Kirkwood JK, Cunningham AA (1994) Epidemiological observations on spongiform encephalopathies in captive wild animals in the British Isles. *Vet Rec* 135(13):296–303.
- [7] Kuwata K, Nishida N, Matsumoto T, Kamatari YO, Hosokawa-Muto J, Kodama K, Nakamura HK, Kimura K, Kawasaki M, Takakura Y, Shirabe S, Takata J, Kataoka Y, Katamine S (2007) Hot spots in prion protein for pathogenic conversion. *Proc Natl Acad Sci USA* 104(29):11921–6.
- [8] Lysek DA (2003) NMR studies of the structure and function of PrP^C, using recombinant prion protein. PHD thesis of Swiss Federal Institute of Technology Zurich.
- [9] Lysek DA, Nivon LG, Wüthrich K (2004) Amino acid sequence of the *Felis catus* prion protein. *Gene* 341:249–53.

- [10] Lysek DA, Schorn C, Nivon LG, Esteve-Moya V, Christen B, Calzolari L, von Schroetter C, Fiorito F, Herrmann T, Gntert P, Wüthrich K (2005) Prion protein NMR structures of cats, dogs, pigs, and sheep. *Proc Natl Acad Sci USA* 102(3):640–5.
- [11] Nyström S, Hammarström P (2015) Generic amyloidogenicity of mammalian prion proteins from species susceptible and resistant to prions. *Sci Rep* 5:10101. doi: 10.1038/srep10101.
- [12] Onizuka K (2009) Dogs never gets prion diseases. The entropic landscape analysis of prion proteins answers why. *Nature Precedings* hdl:10101/npre.2009.3043.1.
- [13] Polymenidou M, Trusheim H, Stallmach L, Moos R, Julius C, Miele G, Lenz-Bauer C, Aguzzi A (2008) Canine MDCK cell lines are refractory to infection with human and mouse prions. *Vaccine* 26(21):2601–14.
- [14] Qing LL, Zhao H, Liu LL (2014) Progress on low susceptibility mechanisms of transmissible spongiform encephalopathies. *Dongwuxue Yanjiu* 35(5):436–45.
- [15] Sanchez-Garcia J, Jensen K, Zhang Y, Rincon-Limas DE, Fernandez-Funez P (2016) A single amino acid (Asp159) from the dog prion protein suppresses the toxicity of the mouse prion protein in *Drosophila*. *Neurobiol Dis* 95:204–9.
- [16] Vidal E, Fernández-Borges N, Pintado B, Ordóñez M, Márquez M, Fondevila D, Torres JM, Pumarola M, Castilla J (2013) Bovine spongiform encephalopathy induces misfolding of alleged prion-resistant species cellular prion protein without altering its pathobiological features. *J Neurosci* 33(18):7778–86.
- [17] Vorberg I, Groschup MH, Pfaff E, Priola SA (2003) Multiple amino acid residues within the rabbit prion protein inhibit formation of its abnormal isoform. *J Virol* 77(3):2003–9.
- [18] Wan J, Bai X, Liu W, Xu J, Xu M, Gao H (2009) Polymorphism of prion protein gene in Arctic fox (*Vulpes lagopus*). *Mol Biol Rep* 36(6):1299–303.
- [19] Wopfner F, Weidenhöfer G, Schneider R, von Brunn A, Gilch S, Schwarz TF, Werner T, Schätzl HM (1999) Analysis of 27 mammalian and 9 avian PrPs reveals high conservation of flexible regions of the prion protein. *J Mol Biol* 289(5):1163–78.
- [20] Wu C, Pang W, Yang J, Zhou X, Zhao D (2006) Amino acid sequence of the Pekingese dog prion protein gene. *Xenotransplantation* 13(5):471–4.
- [21] Zhang JP (2012) The nature of the infectious agents: PrP models of resistant species to prion diseases (dog, rabbit and horses), in *Prions and Prion Diseases: New Developments*, Editor Jean-Michel Verdier, NOVA Publishers, 2012 2nd Quarter, ISBN 978–1–62100–027–3 (print), Chapter 2, pp. 41–8.
- [22] Zhang JP (2015) *Molecular Structures and Structural Dynamics of Prion Proteins and Prions - Mechanism Underlying the Resistance to Prion Diseases*, Springer, ISBN 978–94–017–7317–1, doi: 10.1007/978-94-017-7318-8.

- [23] Zhang J, Liu DD (2011) Molecular dynamics studies on the structural stability of wild-type dog prion protein. *J Biomol Struct Dyn* 28(6):861–9.
- [24] Zhang Z, Wang R, Xu L, Yuan F, Zhou X, Yang L, Yin X, Xu B, Zhao D (2013) Molecular cloning and sequence analysis of prion protein gene in Xiji donkey in China. *Gene* 529(2):345–50.
- [25] Zhang JP, Wang F, Zhang YL (2015) Molecular dynamics studies on the NMR structures of rabbit prion protein wild type and mutants: surface electrostatic charge distributions. *J Biomol Struct Dyn* 33(6):1326–35.

Table 2: All HBs of the D159N mutant and of the wild-type at 300 K, under neutral pH environment during the whole 30 ns' MD simulations:

Hydrogen bonds (HBs)	D159N mutant (% occupied rate)	Wild-type (% occupied rate)
T188@O-T192@HG1	89.69	90.84
C179@O-Y183@HG1	86.21	89.55
D178@OD1-R+164@HE	13.13	54.05
D178@OD2-R+164@HH21	9.18	52.07
D178@OD1-R+164@HH21	6.95	38.84
D202@OD2-R+156@HH21		46.46
D202@OD1-R+156@HH21		38.87
D202@OD1-R+156@HE		37.73
D202@OD2-R+156@HE		17.25
D202@OD1-Y157@HH	9.74	53.98
D202@OD2-T199@HG1		41.63
D202@OD1-T199@HG1		13.73
D202@OD2-Y149@HH		24.72
D202@OD1-Y149@HH		17.85
H+187@O-T191@HG1	71.25	84.35
Y149@O-N153@HD21		17.46
Q212@O-T216@HG1	48.43	81.55
Q227@OE1-Q212@HE21		13.29
Q212@OE1-Q227@HE21		9.74
D147@OD1-R+151@HH12	7.00	26.35
D147@OD1-R+151@HH11	6.75	24.47
D147@OD2-H+140@HD1	16.73	26.46
D144@OD1-R+151@HH12		11.39
V189@O-T193@HG1	21.28	32.71
E211@OE2-R+177@HH21	11.91	15.17
E211@OE1-R+177@HH21	8.41	18.94
E211@OE2-R+177@HE		29.98
E211@OE1-R+177@HE		26.05
E211@OE1-R+177@HH12		8.71
E207@OE2-R+177@HH22	6.55	10.69
E207@OE1-R+177@HH22	5.21	14.15
E207@OE1-R+177@HH12		6.57
E223@O-R+228@HH21		10.76
E223@O-R+228@HE		11.24
E223@O-R+228@HH11		7.45
E223@O-Q219@HE22		13.09
E146@OE2-K+204@HZ2	6.34	18.46
E146@OE2-K+204@HZ1	5.96	16.90
E146@OE1-K+204@HZ2	5.94	17.65
E146@OE2-K+204@HZ3	5.69	15.90
E146@OE1-K+204@HZ3	5.54	15.75
E146@OE1-K+204@HZ1	5.31	16.76
Q219@OE1-Q227@HE22		24.37
Q227@OE1-Q219@HE22		5.71
T216@OG1-Q227@HE21		6.78
S231@OG-N171@HD22		9.12
G229@O-N171@HD21		28.10
H+140@O-R+208@HH21		22.37
H+140@O-R+208@HE		11.59
P158@O-R+136@HH12		15.63
V176@O-Y218@HH		14.65
D178@OD1-Y128@HH		8.95
Q186@OE1-Y128@HH		8.62
S132@OG-Q217@HE21		7.61
N174@OD1-Q172@HE22		7.36
A224@O-R+228@HH11		6.95
Y225@O-R+228@HE		6.63
N197@O-R+156@HH22		6.33
E196@OE2-R+156@HH12		5.33